

## SECULAR VARIATION OF $\Delta^{14}\text{C}$ DURING THE MEDIEVAL SOLAR MAXIMUM: A PROGRESS REPORT

P. E. DAMON,<sup>1</sup> C. J. EASTOE,<sup>1</sup> M. K. HUGHES,<sup>2</sup> R. M. KALIN,<sup>3</sup> A. LONG<sup>1</sup> and  
A. N. PERISTYKH<sup>1</sup>

**ABSTRACT.** The Earth is within the Contemporaneous Solar Maximum (CSM), analogous to the Medieval Solar Maximum (MSM). If this analogy is valid, solar activity will continue to increase well into the 21st century. We have completed 75 single-ring and 10 double-ring measurements from AD 1065 to AD 1150 to obtain information about solar activity during this postulated analog to solar activity during the MSM.  $\Delta^{14}\text{C}$  decreases steadily during the period AD 1065 to AD 1150 but with cyclical oscillations around the decreasing trend. These oscillations can be successfully modeled by four cycles. These four frequencies are  $1/52 \text{ yr}^{-1}$ ,  $1/22 \text{ yr}^{-1}$ ,  $1/11 \text{ yr}^{-1}$ , and  $1/5.5 \text{ yr}$ , *i.e.*, the 4th harmonic of the Suess cycle, the Hale and Schwabe cycles and the 2nd harmonic of the Schwabe cycle.

### INTRODUCTION

We were motivated to make single-year measurements on cellulose extracted from single-year tree rings for the Medieval Solar Maximum (MSM, AD 1100–1250) after reading a paper by Raisbeck *et al.* (1990). Their Figures 2 and 3 show that 20th century  $^{10}\text{Be}$  concentrations  $C_{10}$  ( $^{10}\text{Be}$  a/g) have decreased to the level observed during the MSM. It is well known that 20th century solar activity has been increasing and it has been suggested that the MSM may be a good analogy to the Contemporaneous Solar Maximum (CSM) (Jirikowic and Damon 1994). If so, high solar activity may continue into the 21st century. Since starting this project, we have decided to continue single-year measurements to complete the gap between our measurements and the beginning of the Seattle single-year measurements (AD 1510–1954; Stuiver and Braziunas 1993).

Figure 1 is slightly modified after Raisbeck *et al.* (1990). The  $^{10}\text{Be}$  data ( $C_{10}$ ) are from a 127-m ice core drilled at the South Pole that is relatively free of the extreme meteorological variability experienced in the Arctic. For example, Figure 2 shows the  $C_{10}$  data from Beer *et al.* (1994) for the Dye 3 core (65.2°N, 43.8°W), Greenland. Lal (1987) and Monaghan (1987) have pointed out that the  $^{10}\text{Be}$  production rate variations during major solar minima such as the Maunder Minima and Spörer Minima are dominated by meteorological factors. Damon, Peristykh and Meese (1997) have shown that this is also true for the Schwabe and Hale cycle. It should be kept in mind that the accumulation rate of ice ( $A$ ) enters into  $C_{10}$ , *i.e.*,  $C_{10}$  (a/g) is equal to  $F_{10}$  (a/cm<sup>2</sup>yr) divided by  $A$ :

$$C_{10}(\text{a/g}) = \frac{F_{10}(\text{a/cm}^2 \text{yr})}{A(\text{g/cm}^2 \text{yr})} .$$

Even if  $A$  is known and  $F_{10}$  is calculated,  $F_{10}$  may vary due to more or less  $^{10}\text{Be}$  fallout before reaching the site of deposition. According to Lal (1987) the fallout latitudinal effect independently of  $A$  or production rate can lead to a large variability in the latitudinal fallout of stratospheric  $^{10}\text{Be}$ . For example,  $^{90}\text{Sr}$  fallout changed from 31% to 10% in going from 70°N to 78°N. There is a remarkable contrast between the South Pole  $C_{10}$  record, where  $^{10}\text{Be}$  is concentrated primarily by direct condensation from the polar troposphere, and the  $C_{10}$  record from Dye 3, where  $^{10}\text{Be}$  fallout is subject to the vicissitudes of a more complex weather system. There is little correspondence between the  $\Delta^{14}\text{C}$  record from tree rings and Dye 3  $C_{10}$ .

<sup>1</sup>Laboratory of Isotope Geochemistry, Department of Geosciences, The University of Arizona, Tucson, Arizona 85721

<sup>2</sup>Laboratory of Tree-Ring Research, The University of Arizona, Tucson, Arizona 85721

<sup>3</sup>Department of Civil Engineering, The Queen's University of Belfast, Belfast BT7 1NN, Northern Ireland

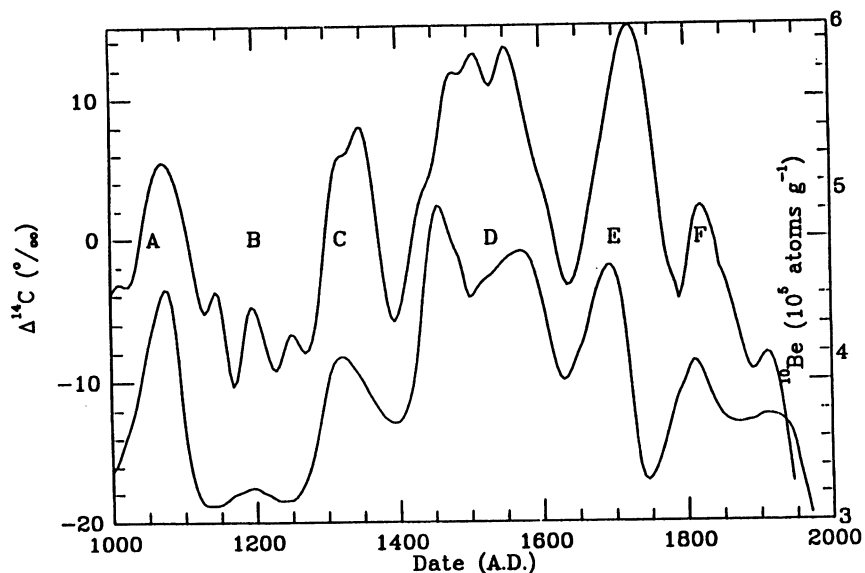


Fig. 1.  $\Delta^{14}\text{C}$  and  $^{10}\text{Be}$  vs. time. The fine structure of  $\Delta^{14}\text{C}$  and  $^{10}\text{Be}$  concentrations in South Pole ice (Raisbeck *et al.* 1990) varies inversely with historic solar activity events. A = Oort Minimum; B = Medieval Solar Activity Maximum; C = Wolf Minimum; D = Spörer Minimum; E = Maunder Minimum; F = Dalton Minimum.

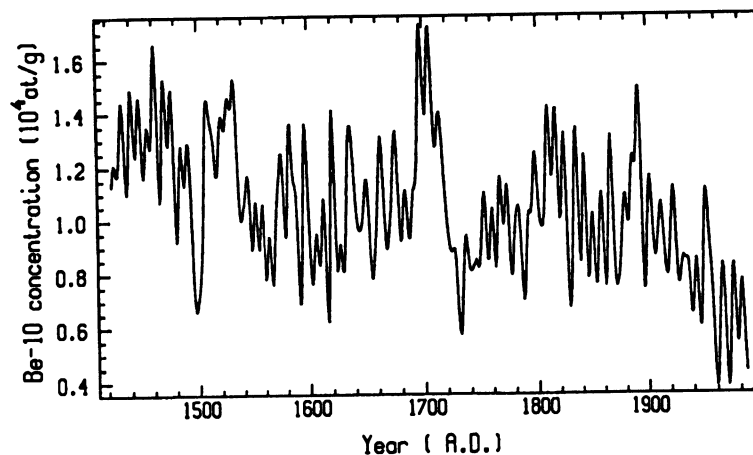


Fig. 2.  $^{10}\text{Be}$  (a/g) in the Dye 3 polar core from Greenland (Beer *et al.* 1994). Note the lack of correspondence to Fig. 1 resulting from meteorological factors.

Notwithstanding the complexity of the meteorological cycle effects on  $\text{C}_{10}$  and to a lesser but significant extent on  $\text{F}_{10}$ , Beer *et al.* (1990) state, "Despite the short term fluctuations caused by transport and deposition effects,  $^{10}\text{Be}$  turns out to be the most promising cosmogenic radioisotope with which to detect the 11-yr Schwabe cycle." The Be cycle looks simple, as shown in Figure 10 of McHargue and Damon (1991), but as we have pointed out it is very complex. On the other hand, the carbon cycle acts as a low-pass filter because the atmosphere contains *ca.* 110 times the average annual production rate of  $^{14}\text{C}$ . Hence, if the production rate is doubled for one year,  $\Delta^{14}\text{C}$  will increase by only

9‰. An 11-yr cycle will be attenuated by a factor of 58 with reference to the Fourier transform of the box diffusion model, with an added sedimentary sink added to balance the production rate with the decay rate (see Figures 1 and 3 of Damon *et al.* 1983 for Fourier transform). However, the precision of  $\Delta^{14}\text{C}$  measurement is  $\pm 2\text{‰}$ , compared with 40‰ to 100‰ for  $^{10}\text{Be}$  measurements (Beer *et al.* 1990). Thus, the fact that the carbon cycle acts as a low-pass filter is compensated by the high precision obtainable in measuring  $\Delta^{14}\text{C}$ . Furthermore, the irradiance component of solar activity is synchronous with the solar wind changes and, because the diffusion rates of atoms and heat into the mixed layer of the ocean are similar,  $\Delta^{14}\text{C}$  provides a good measure of total solar activity. For example, the increase in  $\Delta^{14}\text{C}$  during the Maunder Minimum seems to be a 50/50 result of 1) decreased irradiance decreasing the transfer of carbon from the troposphere to the mixed layer of the ocean and 2) increased production of  $^{14}\text{C}$  with the weakening of the magnetic field embedded in the solar wind (Damon and Sonett 1991). Consequently, we conclude that despite the low-pass filter effect,  $\Delta^{14}\text{C}$  measured from the cellulose of dendrochronologically dated tree rings provides the best measure of total solar activity, whereas  $^{10}\text{Be}$  in Arctic ice may be more useful for interpreting the meteorological record.

## METHODOLOGY

We are in the process of analyzing annual tree-ring samples for the period of time from AD 1065 to AD 1250. This period of time encompasses the Medieval Solar Maximum. The dendrochronologically dated tree-ring samples from the Sequoia National Forest (36°44'N, 118°58'W) were divided into single-year samples under the supervision of Dr. Ramzi Touchan. This work was done in the Laboratory of Tree-Ring Research at the University of Arizona.

The cellulose preparation and  $^{14}\text{C}$  analysis were carried out in the Laboratory of Isotope Geochemistry. Each cellulose sample was converted to 7 g (8 mL) of pure benzene and counted in a LKB Quantulus™ spectrometer 10 m underground. Initially, low-K borosilicate vials were used. We now use 10 mL quartz glass vials made by the University of Waikato, New Zealand. The standard sample is HOxI. The following counting characteristics were obtained:

	Silica	Borosilicate
Background	0.3789 $\pm$ 0.0031 cpm	0.9528 $\pm$ 0.0245 cpm
Standard	62.7984 $\pm$ 0.0469 cpm	67.4776 $\pm$ 0.0611 cpm
Figure of Merit ( $S^2/B$ )	10,410	4,780

The lower count rate for the standard using the “quartz” vials results from the choice of a narrower counting window. However, this does not significantly contribute to the much lower background.

We have observed one significant increase in background that affected three of the consecutive samples shown in Figure 3 (AD 1147, 1149, 1150) as well as a nonconsecutive set not included in Figure 3. The shift was from  $0.3811 \pm 0.0038$  to  $0.4334 \pm 0.0037$ . Appropriate corrections were made.

## RESULTS

We have completed consecutive analyses from AD 1065 to 1150. Seventy-five of the analyses are from single-year tree-ring samples and ten, where insufficient wood was available, are from two-year samples.

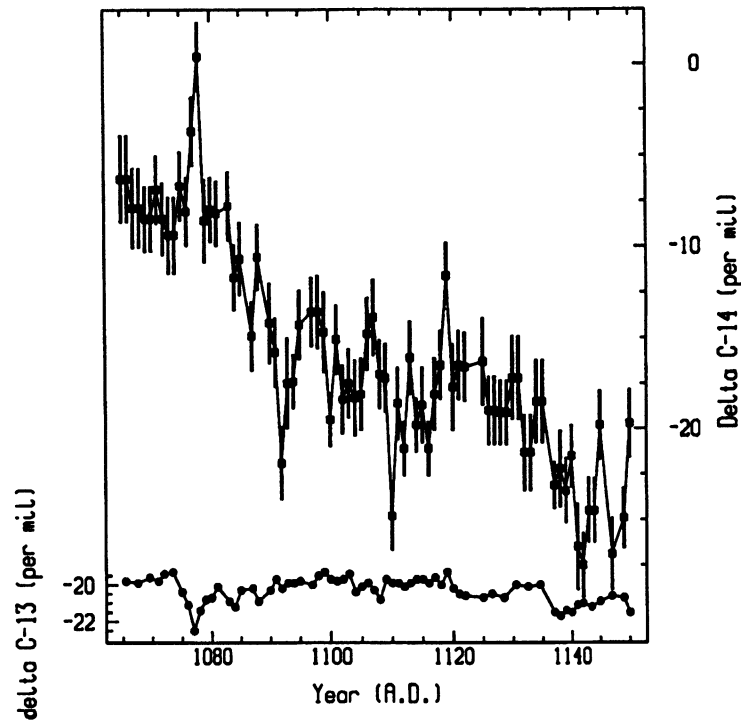
Fig. 3. Measured data,  $\Delta^{14}\text{C}$  and  $\delta^{13}\text{C}$ 

Table 1 shows a comparison of averages of annual  $\Delta^{14}\text{C}$  measurements for the nine decades from AD 1065 to AD 1145. It can be seen from Table 1 that the mean difference is  $-1.0 \pm 2.1\%$ . If we eliminate the AD 1135 decade that deviates by  $>3\sigma$  from the mean, the mean difference becomes  $-0.4 \pm 1.3 (\sigma) \%$ . These results demonstrate that there is no significant calibration difference or regional difference between these two sets of data.

TABLE 1. Comparison of Decadal  $\Delta^{14}\text{C}$ , Tucson vs. Seattle

Decade AD	Tucson (‰)	Seattle (‰)	D = (T) - (S) (‰)
1065	-7.6	-9.1	1.5
1075	-6.9	-7.6	0.7
1085	-11.2	-10.8	-0.4
1095	-16.5	-15.5	-1.0
1105	-17.5	-17.0	0.5
1115	-17.9	-17.9	0.0
1125	-17.9	-14.8	-3.1
1135	-20.8	-15.2	-5.6
1145	-24.3	-23.9	-0.4

$\bar{D} = -1.0$   
 $\sigma_{n-1} = \pm 2.1 (\sigma)$

Figure 3 is a plot of the data from AD 1065 to AD 1150. The record begins with the Oort Minimum averaging *ca.*  $-7\%$  from AD 1065 to AD 1083. Following the Oort Minimum,  $\Delta^{14}\text{C}$  decreases as solar activity increases by *ca.*  $10.5\%$  at AD 1100 and oscillates around  $-17.5\%$  until AD 1135, after which  $\Delta^{14}\text{C}$  decreases  $8.1\%$  to an average of  $-26.6\%$  between AD 1141 and 1144. A similar decrease is evident in the Stuiver and Becker (1993) decadal data. Their data show a decrease of  $8.7\%$  from the AD 1135 decade to the AD 1145 decade. The decadal data of Stuiver and Becker show that this minimum is not sustained and  $\Delta^{14}\text{C}$  returns to higher previous values in the AD 1155 decade. During the Oort Minimum there is a sharp rise in  $\Delta^{14}\text{C}$  for two years, AD 1077–1078, accompanied by a decrease in  $\delta^{13}\text{C}$ . This may possibly be explained by a decrease in upwelling of  $^{14}\text{C}$ -depleted  $\text{CO}_2$  that occurs along the Pacific Coast of California (Damon *et al.* 1989; Damon 1995; McCormac *et al.* 1995; Southon and Baumgartner 1996). The upwelling  $^{14}\text{C}$ -depleted  $\text{CO}_2$  must have  $\delta^{13}\text{C}$  heavier than  $-7\%$  to explain the decrease in  $\delta^{13}\text{C}$  with increase in  $\Delta^{14}\text{C}$ . We plan to test this hypothesis.

The dashed line in Figure 4 suggests a steady increase in solar activity with consequent decrease in  $\Delta^{14}\text{C}$ , but with what appear to be periodic or quasi-periodic oscillations about the declining trend. The oscillations are revealed by a Rönische spline with 95% pass at 22 yr. A cycle of *ca.* 50 yr is evident, accompanied by variations of higher frequency. Upon removing the linear trend from the raw data, the DFT in Figure 5 is obtained. The DFT shows a *ca.* 51-yr peak with high amplitude and higher frequency peaks close to the Hale and Schwabe cycles with second and fourth harmonics. A good approximation to the raw signal can be obtained by assuming the presence of four idealized cycles around the trend curve (Fig. 6). These cycles are 52 yr, 22 yr, 11 yr and 5.5 yr. These represent the fourth harmonic of the Suess cycle (Damon and Jirikowic 1992), the Hale cycle and the Schwabe cycle with its second harmonic. The fit to the idealized curve is remarkably good. All but five anomalous data points can be accounted for by measurement errors alone.

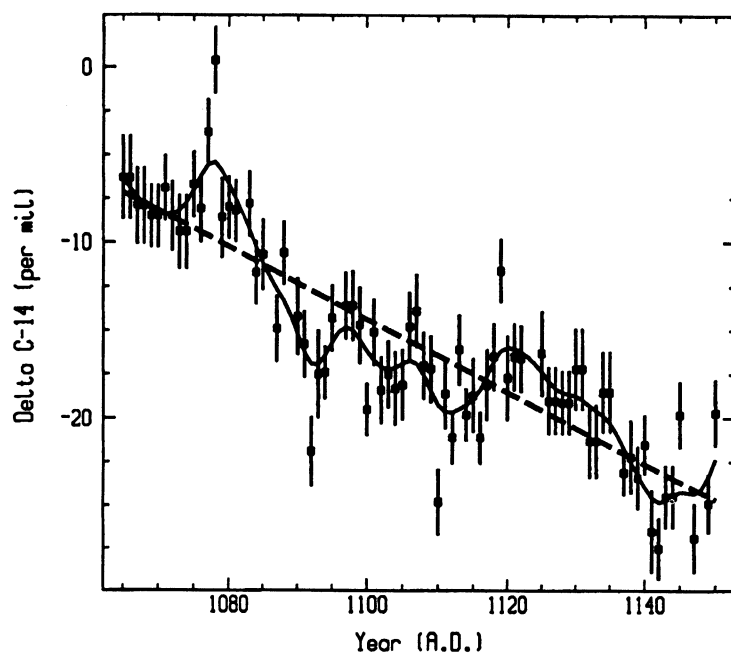


Fig. 4. Measured  $^{14}\text{C}$  data ( $\blacksquare = \pm 1 \sigma$  error bars) with linear trend (---). The bold curve is a Rönische spline with 95% pass at 22 yr.

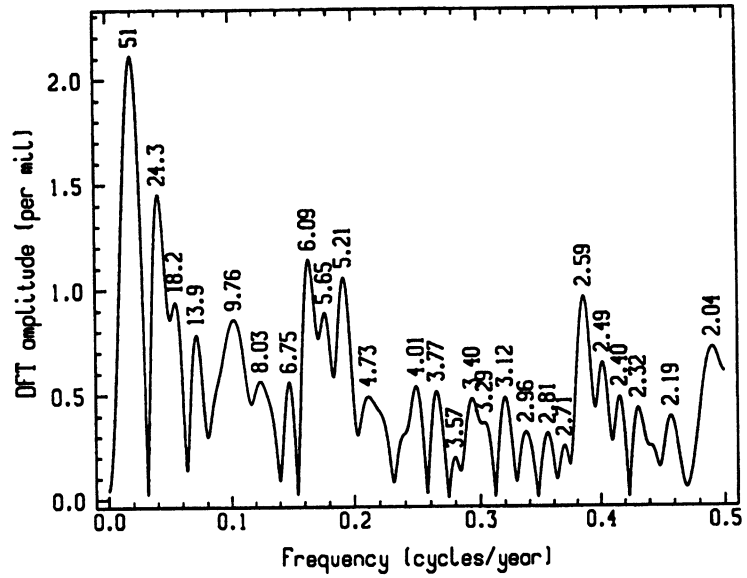


Fig. 5. Amplitude of DFT power spectrum after linear detrend

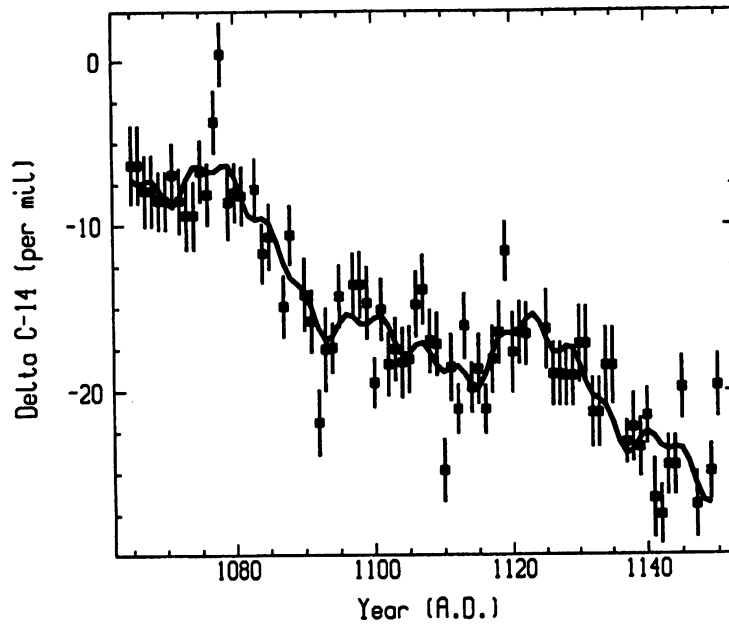


Fig. 6. Measured data model by four frequencies ( $1/52 \text{ yr}^{-1}$ ,  $1/22 \text{ yr}^{-1}$ ,  $1/11 \text{ yr}^{-1}$  and  $2/11 \text{ yr}^{-1}$ ). Amplitudes of these cycles are obtained by harmonic regression.

## CONCLUSION

The following conclusions seem to be warranted by our analysis:

1. There appears to be no calibration or regional difference between the Tucson and Seattle data, both of which are for tree-ring samples from North American marine west coast localities.
2. Following the Oort Minimum,  $\Delta^{14}\text{C}$  declines by *ca.* 20‰ by AD 1150 as solar activity increases. Adding the effect of the declining geomagnetic dipole moment would add only *ca.* 0.5‰.
3. The data can be modeled by harmonic regression around a declining linear trend. Only four frequencies are required:  $1/52 \text{ yr}^{-1}$ ,  $1/22 \text{ yr}^{-1}$ ,  $1/11 \text{ yr}^{-1}$  and  $2/11 \text{ yr}^{-1}$ . Only five of the outlying data points cannot be explained by the measurement error. The  $1/52 \text{ yr}^{-1}$  frequency is the fourth harmonic of the Suess cycle  $1/208$  (Damon and Jirikowic 1992).
4. The increased solar activity during the Medieval Solar Maximum is similar to the observed increase during the Contemporaneous Modern Solar Maximum. If the MSM is a good analog to the CSM, then the decadal data of Stuiver and Becker (1993) suggest that the CSM may continue into the 21st century.

## ACKNOWLEDGMENTS

The authors thank Dr. Ramzi Touchan and Mr. John J. Manes for preparation of the tree-ring samples. This work was supported by NSF Grant ATM-9520135 and the State of Arizona.

## REFERENCES

- Beer, J., Baumgartner, St., Dittrich-Hannen, B., Hauenstein, J., Kubik, P., Lukaszczuk, C., Mende, W., Stellmacher, R. and Suter, M. 1994 Solar variability traced by cosmogenic isotopes. In Pap, J. M., Fröhlich, C., Hudson, H. S. and Solanki, S. K., eds., *The Sun as a Variable Star: Solar and Stellar Irradiance Variations*. Cambridge, Cambridge University Press: 291–300.
- Damon, P. E. 1995 A note concerning “Location-dependent differences in the  $^{14}\text{C}$  content of wood” by McCormac *et al.* In Cook, G. T., Harkness, D. D., Miller, B. F. and Scott, E. M., eds., Proceedings of the 15th International  $^{14}\text{C}$  Conference. *Radiocarbon* 37(2): 829–830.
- Damon, P. E., Cheng, S. and Linick, T. W. 1989 Fine and hyperfine structure in the spectrum of secular variations of atmospheric  $^{14}\text{C}$ . In Long, A., Kra, R. S. and Srdoč, D., eds., Proceedings of the 13th International  $^{14}\text{C}$  Conference. *Radiocarbon* 31(3): 704–718.
- Damon, P. E. and Jirikowic, J. L. 1992 The Sun as a low-frequency harmonic oscillator. *Radiocarbon* 34(2): 199–205.
- Damon, P. E., Lerman, J. C. and Long, A. 1978 Temporal fluctuations of atmospheric  $^{14}\text{C}$ : Causal factors and implications. *Annual Review of Earth and Planetary Sciences* 6: 457–494.
- Damon, P. E., Peristykh, A. N. and Meese, D. A. (ms.) 1997  $^{10}\text{Be}$  a/g: Production or accumulation? Paper presented at the 8th Scientific Assembly of IAGA, August 4–15, 1997, Uppsala, Sweden. Abstracts with Programs, p. 191. (Manuscript in preparation for *Journal of Geophysical Research*.)
- Damon, P. E., Sternberg, R. S. and Radnell, C. J. 1983 Modeling of atmospheric radiocarbon fluctuations for the past three centuries. In Stuiver, M. and Kra, R. S., eds., Proceedings of the 11th International  $^{14}\text{C}$  Conference. *Radiocarbon* 25(2): 249–258.
- Damon, P. E. and Sonett, C. P. 1991 Solar and terrestrial components of the atmospheric  $\Delta^{14}\text{C}$  variation spectrum. In Sonett, C. P., Giampapa, M. S. and Mathews, M. S., eds., *The Sun in Time*. Tucson, University of Arizona Press: 360–388.
- Jirikowic, J. L. and Damon, P. E. 1994 The medieval solar activity maximum. *Climatic Change* 26: 309–316.
- Lal, D. 1987  $^{10}\text{Be}$  in polar ice: Data reflect changes in cosmic ray flux or polar meteorology. *Geophysical Research Letters* 14(8): 785–788.
- McHargue, L. R. and Damon, P. E. 1991 The global beryllium 10 cycle. *Reviews of Geophysics* 29: 141–158.
- McCormac, F. G., Baillie, M. G. U., Pilcher, J. R. and Kalin, R. M. 1995 Location-dependent differences in the  $^{14}\text{C}$  content of wood. In Cook, G. T., Harkness, D. D., Miller, B. F. and Scott, E. M., eds., Proceedings of the 15th International  $^{14}\text{C}$  Conference. *Radiocarbon* 37(2): 395–407.
- Monaghan, M. C. 1987 Greenland ice  $^{10}\text{Be}$  concentrations and average precipitation rates north of  $40^\circ\text{N}$  to  $45^\circ\text{N}$ . *Earth and Planetary Science Letters* 84: 197–203.
- Raisbeck, G. M., Yiou, F., Jouzel, J. and Petit, J. R. 1990  $^{10}\text{Be}$  and  $\delta^2\text{H}$  in polar ice cores as a probe of the solar variability's influence on climate. In Pecker, J.-C. and

- Runcorn, S. K., eds., *The Earth's Climate and Variability of the Sun over Recent Millennia: Geophysical, Astronomical and Archaeological Aspects*. London, The Royal Society: 65–71.
- Southon, J. R. and Baumgartner, T. A. 1996 A long-term record of upwelling from the Santa Barbara Basin, Southern California [abstract]. AMS-7: Abstracts of the 7th International Conference on Accelerator Mass Spectrometry. *Radiocarbon* 38(1): 114.
- Stuiver, M. and Becker, B. 1993 High-precision decadal calibration of the radiocarbon time scale, AD 1950–6000 BC. In Stuiver, M., Long, A. and Kra, R. S., eds., Calibration 1993. *Radiocarbon* 35(1): 35–65.
- Stuiver, M. and Braziunas, T. F. 1993 Sun, ocean, climate and atmospheric  $^{14}\text{CO}_2$ : An evaluation of causal and spectral relationships. *The Holocene* 3: 289–305.